

SAND97-8236 • UC-704  
Unlimited Release  
Printed February 1997

# The Reapplication of Energetic Materials as Boiler Fuels

S.G. Buckley, G.C. Sclipa, J.R. Ross, C.J. Morey, L.L. Baxter

Prepared by  
Sandia National Laboratories  
Albuquerque, New Mexico 87185 and Livermore, California 94551  
for the United States Department of Energy  
under Contract DE-AC04-94AL85000

Approved for public release; distribution is unlimited.



Issued by Sandia National Laboratories, operated for the United States Department of Energy by Sandia Corporation.

**NOTICE:** This report was prepared as an account of work sponsored by an agency of the United States Government. Neither the United States Government nor any agency thereof, nor any of their employees, nor any of the contractors, subcontractors, or their employees, makes any warranty, express or implied, or assumes any legal liability or responsibility for the accuracy, completeness, or usefulness of any information, apparatus, product, or process disclosed, or represents that its use would not infringe privately owned rights. Reference herein to any specific commercial product, process, or service by trade name, trademark, manufacturer, or otherwise, does not necessarily constitute or imply its endorsement, recommendation, or favoring by the United States Government, any agency thereof or any of their contractors or subcontractors. The views and opinions expressed herein do not necessarily state or reflect those of the United States Government, any agency thereof, or any of their contractors or subcontractors.

This report has been reproduced from the best available copy.

Available to DOE and DOE contractors from:

Office of Scientific and Technical Information  
P.O. Box 62  
Oak Ridge TN 37831

Prices available from (615) 576-8401, FTS 626-8401.

Available to the public from:

National Technical Information Service  
U.S. Department of Commerce  
5285 Port Royal Rd.  
Springfield, VA 22161

SAND97-8236  
Unlimited Release  
Printed February 1997

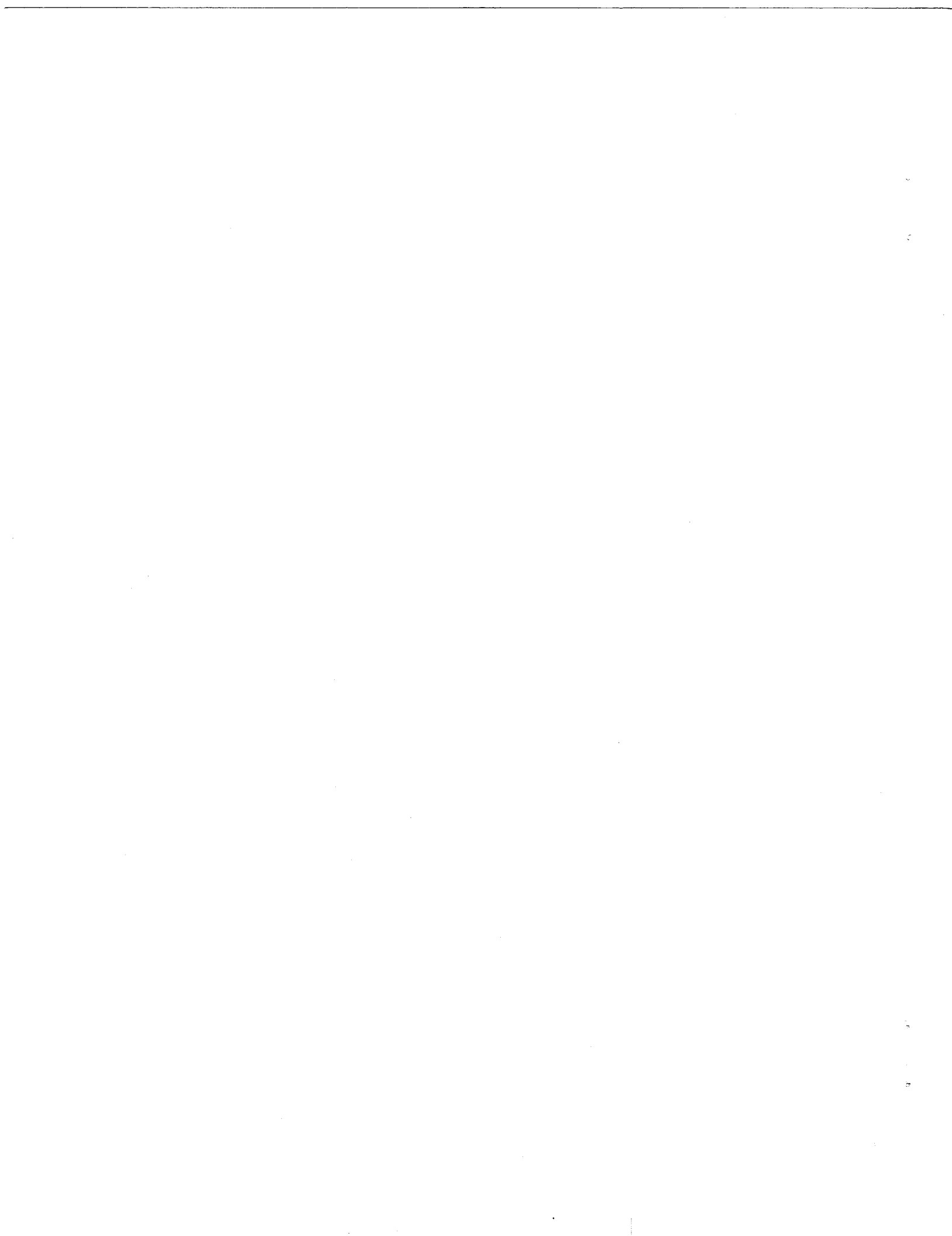
## The Reapplication of Energetic Materials as Boiler Fuels

Steven G. Buckley, Gian C. Sclipa, James R. Ross, Candace J. Morey, Larry L. Baxter

Combustion Research Facility  
Sandia National Laboratories  
Livermore, CA 94551

### ABSTRACT

Decommissioning of weapons stockpiles, off-specification production, and upgrading of weapons systems results in a large amount of energetic materials (EM) such as rocket propellant and primary explosives that need to be recycled or disposed of each year. Presently, large quantities of EM are disposed of in a process known as open-burn/open-detonation (OB/OD), which not only wastes their energy content, but may release large quantities of hazardous material into the environment. Here we investigate the combustion properties of several types of EM to determine the feasibility of reapplication of these materials as boiler fuels, a process that could salvage the energy content of the EM as well as mitigate any potential adverse environmental impact. Reapplication requires pretreatment of the fuels to make them safe to handle and to feed. Double-base nitrocellulose and nitroglycerin, trinitrotoluene (TNT), nitroguanidine, and a rocket propellant binder primarily composed of polybutadiene impregnated with aluminum flakes have been burned in a 100-kW downfired flow reactor. Most of these fuels have high levels of fuel-bound nitrogen, much of it bound in the form of nitrate groups, resulting in high  $\text{NO}_x$  emissions during combustion. We have measured fuel-bound nitrate conversion efficiencies to  $\text{NO}_x$  of up to 80%, suggesting that the nitrate groups do not follow the typical path of fuel nitrogen through HCN leading to  $\text{NO}_x$ , but rather form  $\text{NO}_x$  directly. We show that staged combustion is effective in reducing  $\text{NO}_x$  concentrations in the postcombustion gases by nearly a factor of 3. In the rocket binder, measured aluminum particle temperatures in excess of 1700 °C create high levels of thermal  $\text{NO}_x$ , and also generate concern that molten aluminum particles could potentially damage boiler equipment. Judicious selection of the firing method is thus required for aluminum-containing materials. We conclude that cofiring with a traditional fuel in a boiler is an excellent option for obtaining useful energy from these hazardous materials.



## INTRODUCTION

Significant amounts of energetic materials (EM) await reapplication, reuse, or destruction in the US and abroad. EM is a broad classification including solid rocket propellants and high explosives. The institutions primarily responsible for this material include the United States Department of Defense, Department of Energy, Department of Transportation (Coast Guard), the National Aeronautical and Space Administration, explosives and propellant manufacturing companies, and corresponding institutions in countries other than the US. The sources of this material include reduction of weapon inventories (conventional and nuclear) and manufacturing waste. The bulk of the EM are from the conventional weapons stockpile, of which an estimated 375,000 to 400,000 metric tons are currently awaiting disposal (Arbuckle 1996; Huizinga 1996). The Department of Defense currently plans to spend approximately \$100 million annually to eliminate this backlog by the year 2001, after which generation is expected to average 60,000 metric tons per year (Arbuckle 1996). In addition to storage problems and logistical overhead caused by this stockpile, negotiation of and compliance with arms control agreements with the states of the former Soviet Union are affected by lack of an appropriate means for EM reapplication. It is estimated that approximately 200,000 metric tons of EM await demilitarization in the former Soviet Union (Blixrud 1996). While many disposal technologies are under investigation, including biodegradation, hydrothermal processing, and plasma techniques, no environmentally sound means of disposing of this material are yet available (Wheeler 1996).

The current primary method of EM disposal is termed "open burn/open detonation" (OB/OD), which is the practice of burning and detonation in open fields, typically at military installations at a distance removed from the general public. Despite the relative isolation of the OB/OD sites, detonation shock waves have been known to reflect off of the upper atmosphere and break windows in towns 10-20 miles distant (Sierra 1996). In addition, plumes from the detonation and burning are typically visible for many miles. Because of public and regulatory concerns, OB/OD of these materials is becoming increasingly unacceptable. Recent measurements of emissions from OB/OD of antipersonnel mines indicate that significant quantities of pollutants can be emitted; for example, the emission factors (wt/wt) were  $5.84 \times 10^{-3}$ ,  $8.15 \times 10^{-4}$ , and  $3.06 \times 10^{-3}$  for methane, benzene, and total aromatics, respectively (Wilcox 1996). Other measurements from contained burns of solid rocket motors showed the exhaust to contain roughly 3%

HCl, 100 ppm HCN, 2,500 ppm CH<sub>4</sub>, and 100 ppm of volatile organics (such as chloromethane, benzene, and 1,2 dichloroethane) on a weight basis (Steele 1996).

Given the environmental concerns, and with current disposal costs approximately \$850 per metric ton (Arbuckle 1996), reapplication of this material is highly desirable. Potential reapplication technologies under development include use as explosives in mining and excavation, as well as processing to withdraw high-value commercial chemicals. Some of these processes result in byproducts that could be used as boiler fuels. In addition, the EM can be converted entirely to boiler fuel by desensitization processes, which make the fuel safe to handle and feed. Such treated fuels are hereafter referred to as EM-derived fuels (EMDF). A preliminary assessment of the combustion properties of energetic materials has shown that the concept holds promise (Myler, Bradshaw et al. 1991), but no pilot-scale study has been completed. Revenues from chemical recovery and power generation approximately equal costs of boiler modifications and maintenance of new fuel feedlines (Shah 1994). This suggests that cofiring EMDF in utility boilers could compete with open burning and open detonation if the cost of preparing EMDF could be held below the cost of open burning or open detonation. Many commercial power generation facilities, particularly biomass facilities, are designed to burn a wide variety of materials such as grasses, agricultural wastes, urban wood waste, and coal, and have feed systems that accommodate wide fluctuations in fuel composition and morphology. Cofiring the energetic materials affords the advantage of preexisting pollution control equipment attached to the boiler to mitigate any environmental hazards, as well as the benefit of energy recovery from the EMDF.

Establishing the reapplication of energetic materials as fuels as a viable technology option depends in large part on characterizing the combustion properties of these fuels, which is the focus of this investigation. Most energetic materials contain high concentrations of nitrogen, much of which is in the form of nitrate groups. Thus, in evaluating the combustion properties of EMDF, we particularly look at the issue of NO<sub>x</sub> generation and control, as NO<sub>x</sub> is the primary EPA "criteria pollutant" expected from combustion of these fuels. Finding that fuels with nitrate groups have extremely high NO<sub>x</sub> emissions, we employ staged combustion to show that the NO<sub>x</sub> can be reduced. In addition, rocket-motor-derived fuel has a significant quantity of aluminum dispersed in the fuel. Aluminum burns at extremely high temperatures, and hence we identify dispersion of high-temperature particles and generation of thermal NO<sub>x</sub> as important concerns. Based on these findings, we expect that the choice of burning configuration will

be the most important technical question for combustion of aluminum-containing EMDF in boilers. Finally, we also address fuel handling techniques throughout the paper.

## FUELS

We investigated four different types of EMDF, as shown in Table 1. Readers familiar with energetic materials will recognize the transportation hazard class rating, which is a very common means of identifying EM.

Table 1: Energetic Materials Derived Fuels (EMDF) examined in this study.

EMDF	Form	Composition	Unique Feature	Hazard Class
Double-base nitroglycerin/nitrocellulose	Liquid	30% water, 64% kerosene, 5% energetic materials, 1% surfactant	O-NO <sub>2</sub> bonded to aliphatic carbon	1.1
Trinitrotoluene (TNT)	Liquid	95% toluene, 5% TNT	NO <sub>2</sub> bonded to aromatic carbon	1.1
Nitroguanidine	Liquid	95% fuel oil #2, 5% nitroguanidine	54% nitrogen by mass, 3 C-N bonds, 1 N-NO <sub>2</sub> bond.	1.1
Rocket motor propellant (Thiokol)	Solid	Mostly polybutadiene rubber impregnated with aluminum, small amounts of ammonium perchlorate	Trace fuel nitrogen, high Al concs.	1.3

Some potential combustion issues associated with high explosives and double-base propellants (Class 1.1) can be appreciated by examining their chemical structures, illustrated in Fig. 1. Nitrogen in typical boiler fuels such as coal is dominated by pyrrolic and pyridinic nitrogen structures (also illustrated in the figure), where the nitrogen is bound in a carbon-containing ring (i.e. nitrogen heterocycle). In contrast, the forms of nitrogen in Class 1.1 materials are predominately either nitrate groups or other forms of nitrogen which are external to the ring. RDX and HMX are notable exceptions, having both in-ring nitrogen and nitrate groups, but in each case half of the nitrogen is still in the form of nitrate groups. Among the EMs illustrated in the figure, the weakest chemical bond in the structure is between the nitrate groups and the remaining structure. As material thermally decomposes, nitrate groups are expected to be eliminated first, leading to locally high  $\text{NO}_2$  concentrations. In subsequent reactions, the remaining nitrate groups sometimes form  $\text{N}_2\text{O}$  or similar compounds, which is also expected to form at least one  $\text{NO}_x$  compound under combustion conditions. Nitrogen not associated with nitrate groups is expected to form  $\text{N}_2\text{O}$  or follow traditional gas-phase nitrogen chemistry through  $\text{HCN}$  (Melius 1988; Behrens Jr. 1990; Melius 1990; Behrens Jr. and Bulusu 1991; Behrens Jr. and Bulusu 1992; Behrens Jr. and Bulusu 1992; Cor and Branch 1995).

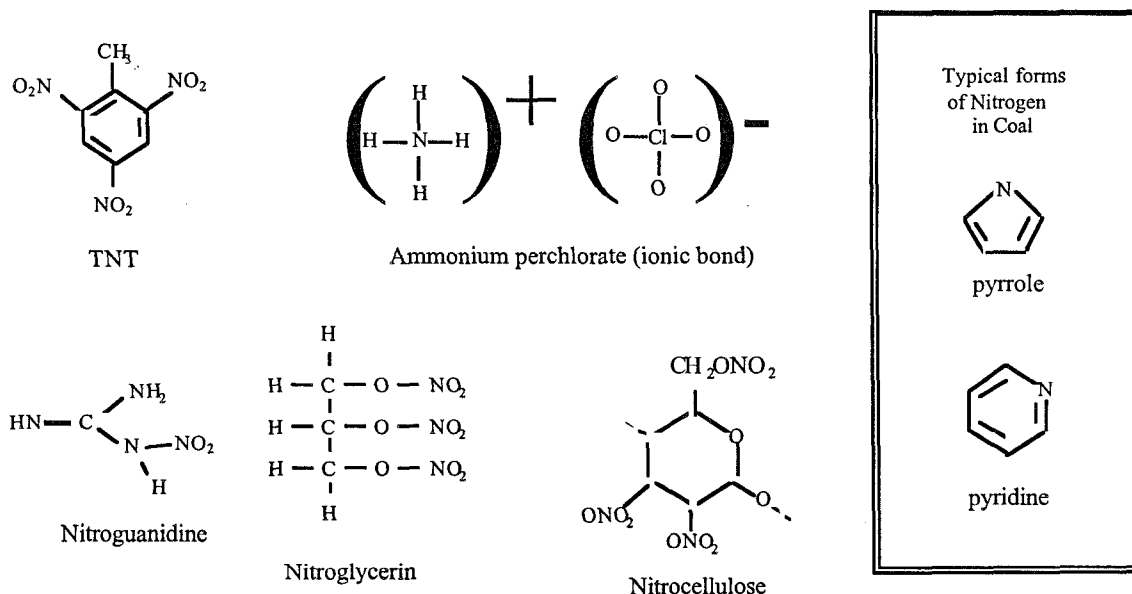


Figure 1. Chemical structures of many energetic materials found in explosives and double-base propellants. Chemical structures for the dominant forms of nitrogen in coal are illustrated for comparison in the box.

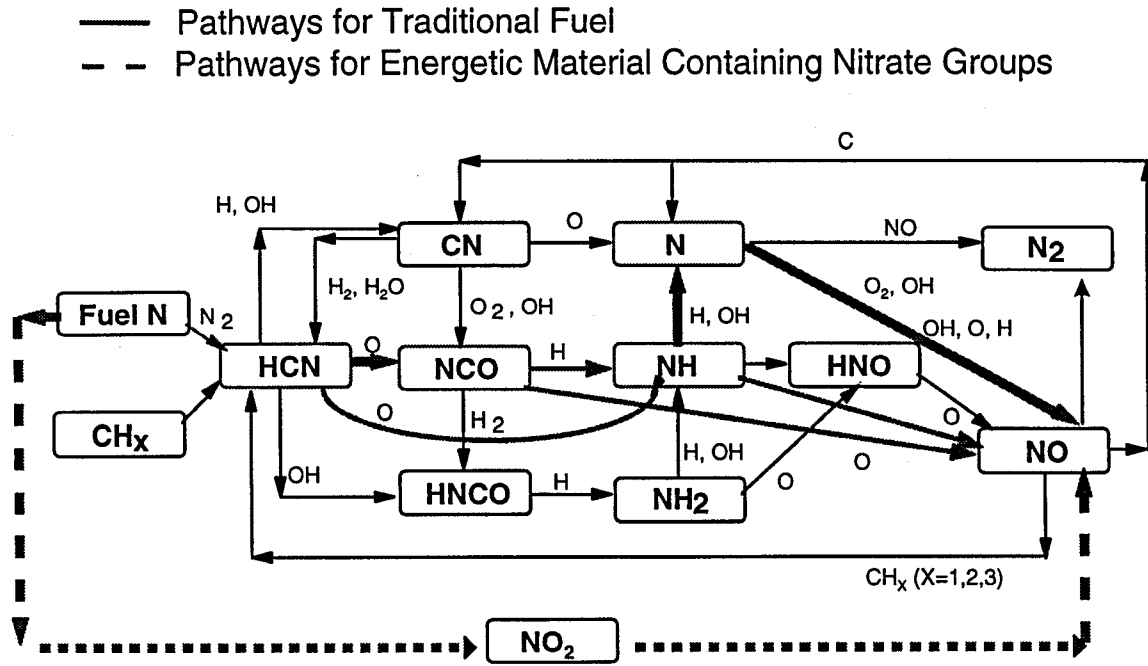


Figure 2. Some of the pathways important for NO<sub>x</sub> formation in combustion systems, showing the direct pathway taken by EMDF containing nitrate groups.

These pathways are illustrated in Fig. 2. The tendency for EMDF to form NO<sub>x</sub> will be shown to be much higher than for traditional fuels, and these chemical differences are believed to be the primary cause of the observed differences.

The solid rocket motor propellant contains nitrogen in the form of residual ammonium perchlorate, NH<sub>4</sub>ClO<sub>4</sub>, which is expected to follow the typical path of fuel-bound nitrogen in combustion chemistry to form predominantly N<sub>2</sub> and NO. The chlorine introduces issues due to the formation of air toxics such as chlorinated hydrocarbons, particularly dioxins, as well as additional soot formation, but these are not directly addressed in this paper. Additionally, the Class 1.3 material contains a high concentration of aluminum, which burns at very high temperatures. This is shown to contribute to thermal NO<sub>x</sub> formation.

Another major difference in the chemical structures of Class 1.1 EM compared with traditional fuels is the high oxygen concentration of the former. These high oxygen contents affect combustion properties such as heating value (Fig. 3), amount of required excess air, stability, and storage. In particular, an evaluation of the worth of EMDF based

on a comparison of standard heating values with typical fuels such as coal can be misleading. Standardized heating value analyses are based on energy content of the fully oxidized material per unit mass of fuel. In the case of EM, most of the oxidizer is contained in the sample. This means that the standard heating value for EM appears to be much lower than that for other fuels, even though the flame temperature, which largely determines the thermodynamic efficiency of an idealized power generation cycle, is often comparable or higher for EMDF.

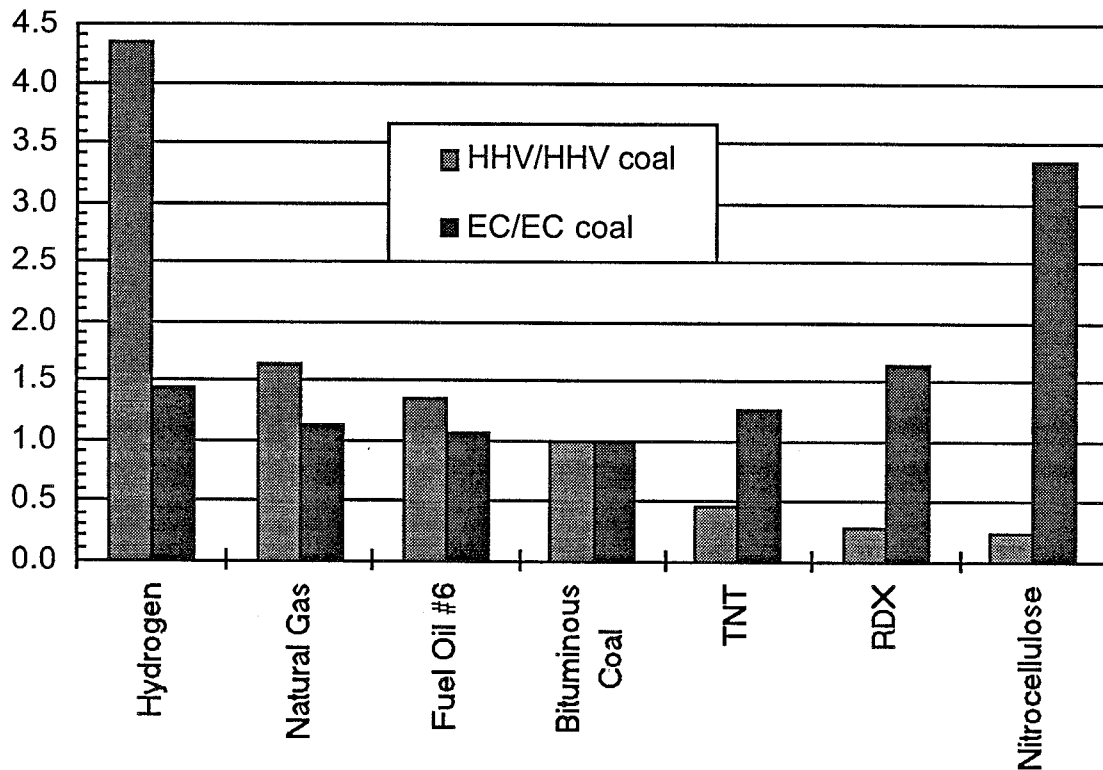


Figure 3. Heating values of traditional fuels compared with energetic materials.

Normalization of the energy content of fuels by the mass of the combustion products provides a more insightful comparison in terms of flame temperatures and other properties that determine usefulness of a fuel in heat engines. Assuming air is used as the oxidizer, values of energy content divided by mass of products for oil and coal are approximately 3.0 and 2.8 MJ/kg, respectively, whereas TNT and RDX are approximately 3.6 and 4.6 MJ/kg, respectively. A comparison of both the traditional

heating value and the energy content (heating value based on total mass of product) is presented in Fig. 3 for selected fuels. The left bar of each set shows the standard higher heating value (HHV) for each fuel normalized to the HHV of coal, while the right bar shows the energy content (EC) of the fuels, normalized by the EC of coal. As shown in the figure, the amount of energy released to the product gas is comparable or higher for EM than for traditional fuels. It follows that EMDFs exhibit flame temperatures that are as high or higher than those for traditional fuels. In practice, EM used as boiler fuels are blended with other components to produce more stable materials, and this mixture would be blended with other fuels to comprise roughly 10% of a fuel stream; hence the impact of these fuels would be a relatively small, but beneficial effect on ideal boiler performance.

## COMBUSTION FACILITIES

The experiments were conducted in the Multifuel Combustor (MFC), illustrated in Fig. 4. The MFC is a small pilot-scale ( $\approx 340$  kW, depending on fuel type) facility that simulates the local environment to which independently injected solid, liquid, or gaseous fuels are exposed as they pass through an entrained-flow combustion system. Fuel is inserted through any of a series of ports along the 4.25-meter length of the combustor, allowing variation of residence time from a few milliseconds to 4-5 seconds. Atop the silicon carbide-lined combustion section is a natural-gas-fired burner, that can be used to control the gas temperature and composition into which fuels are injected; alternately, fuels can be injected directly into the combustor airflow with the burner off, where they may form a self-supporting flame. The combustor wall temperature in each of the modular sections is independently controllable up to 1400 °C in sustained tests. Gas and wall temperatures are measured using type K and R thermocouples, respectively.

Combustion products are extracted from the combustor in a heated line to prevent water condensation, filtered in a heated filter, and measured using analyzers manufactured by Horiba Instruments, including NDIR NO<sub>x</sub>, CO and CO<sub>2</sub> analyzers and a paramagnetic O<sub>2</sub> analyzer.

Unless otherwise specified, data reported here were obtained by firing the fuel in the top section of the MFC and sampling combustion products from the top of the 7<sup>th</sup> section, establishing a 3.7 meter reaction section. Given the 15 cm diameter of the reactor, the 9.44 liter/sec total airflow, and the wall temperature of 900 °C used in most of these tests, the residence time in the reactor was roughly 2.7 seconds. Each of the liquid EMDF were

burned with a reference case of the solvent fuel without the energetic material. The  $\text{NO}_x$  control strategy of staged combustion was accomplished by injecting a second air stream into the top of the 4<sup>th</sup> section, dividing the reactor into an upper fuel-rich section and a lower fuel-lean section. Liquid fuel feeding was accomplished using a positive-displacement cylinder feeder, except in the case of nitroguanidine combustion.

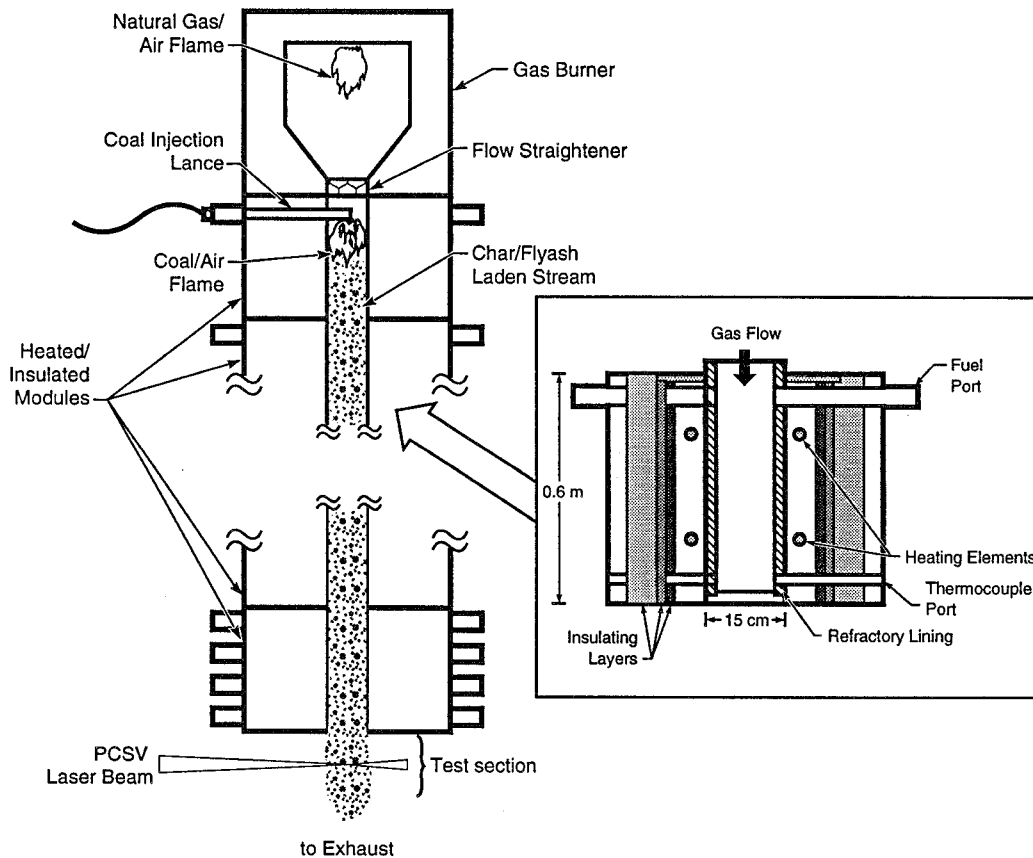


Figure 4. Schematic diagram of Sandia's Multifuel Combustor.

This fuel mixture was difficult to fire, as it would separate within about a minute after mixing. We constructed a pressurized tank with an integral stirring mechanism, which we mounted very close to the point of injection. This eliminated the separation problem, but points to the fuel-handling difficulties that may be encountered with some EMDF. Liquid fuel was sprayed into the combustor with an "atomizing air" flow of roughly 2 liter/sec, downstream of the main "combustion air" flow. The ratio of combustion air to atomizing air determines the shape and mixing parameters of the cone of liquid fuel. A ratio that is too high or too low can result in poor mixing of the fluid streams and unstable

combustion, especially in the case of low atomizing air flowrates; in our experience a ratio in the range of 4-6 yields good mixing. The solid rocket fuel was prepared by cryogenically grinding the fuel and mixing it with utility grind coal (76-200 mesh Black Thunder), which was chosen as a convenient boiler fuel for which the combustion properties are well-known. This was fed using a belt feeder emptying into an eductor, from which the fuel would be transported using high velocity air.

In addition, a limited number of solid rocket fuel combustion experiments were conducted on a low-density mat of alumina fibers suspended in a laminar flow of combustion gases in Sandia's Char Combustion Laboratory (CCL). The captive particle imaging (CPI) system in the CCL monitors individual particle behavior for particles greater than 80- $\mu\text{m}$  diameter. Particle temperature is also monitored throughout the particle combustion history.

## RESULTS AND DISCUSSION

### **NO<sub>x</sub> formation from combustion of EMDF**

Figure 5 presents our measured NO<sub>x</sub> data for the double-base EMDF under different operating conditions and as a function of exit O<sub>2</sub> concentration. Data from the EMDF are compared with data from identically prepared material without EM. The base case (without EM) indicates less than 20-ppmv NO<sub>x</sub> under all conditions, in part due to the large concentration of water in the fuel, which keeps temperatures low. The EMDF, dissolved in the same concentration of kerosene, H<sub>2</sub>O, and surfactant, was fired at two different combustion-air-to-atomizing-air ratios, as indicated, which produces different spray characteristics. NO<sub>x</sub> samples were collected after complete combustion and approximately 1.9-s gas residence time, with a temperature of 800 °C at the collection point. Data are shown on a 3% oxygen basis. The addition of EMDF results in approximately a 50 to 100-fold increase in the NO<sub>x</sub> concentrations, to a maximum of nearly 2000 ppm. Higher NO<sub>x</sub> concentrations are found at higher excess O<sub>2</sub> concentrations, possibly because lower combustion temperatures result in slower kinetics, which are less able to drive the NO<sub>x</sub> concentration toward its equilibrium value of approximately 100 ppm at 900 °C. A minor effect of increasing NO<sub>x</sub> concentrations with higher ratios of combustion air to atomizing air may be due to the better-mixed, more dilute spray (lower ratio) burning more completely.

NO<sub>x</sub> data for 2-4-6 trinitrotoluene (TNT) are shown in Figure 6. The bottom curves show the NO<sub>x</sub> measured at various oxygen concentrations for a base case of pure toluene combustion, while the upper curves show NO<sub>x</sub> measured for combustion of a mixture of 5% (by weight) TNT dissolved in toluene. Figure 6 indicates that the addition of only a small amount of TNT to the fuel dramatically increases the NO<sub>x</sub> emissions, attesting to the efficient conversion of the nitrate (NO<sub>2</sub>) groups of the TNT to NO<sub>x</sub>. The NO<sub>x</sub> generated while firing pure toluene forms through a combination of prompt<sup>1</sup> and thermal<sup>2</sup> mechanisms, and follows expectations, peaking at a few percent oxygen (Miller and Bowman 1989). In contrast, the 5%-TNT fuel adds a significant loading of fuel-bound nitrogen, much of which is converted to nitrogen oxides. This results in both a much higher NO<sub>x</sub> yield and also a yield that is much less dependent on oxygen concentration. Under a range of oxygen conditions, measurements of NO<sub>2</sub> vs NO indicate that NO accounts for over 90% of total NO<sub>x</sub>.

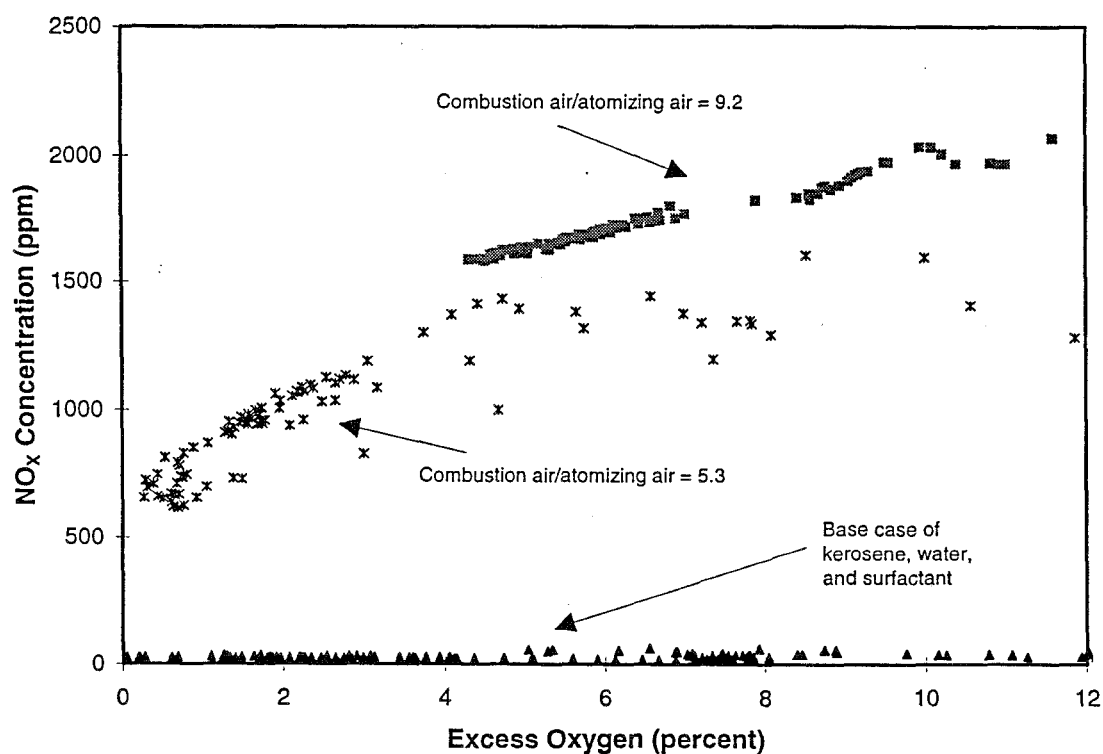


Figure 5. NO<sub>x</sub> emissions from double-base EMDF as a function of exit O<sub>2</sub> concentration, presence of energetic material, and combustion air-to-atomizing air flow rates.

<sup>1</sup> So-called “prompt” NO forms at the flame front from the reaction  $CH+N_2 \Rightarrow HCN + N$ , followed by several possible steps (such as  $N+O_2 \Rightarrow NO + O$ ) which can form NO.

<sup>2</sup> Thermal NO<sub>x</sub> forms from the combination of three reactions:  $N_2 + O \Rightarrow NO + N$ ;  $N + O_2 \Rightarrow NO + O$ ; and  $N + OH \Rightarrow NO + H$ . The first reaction, breaking the N<sub>2</sub> triple bond, has an extremely high activation energy, and so is favored only at high temperatures, giving this mechanism the name “thermal”.

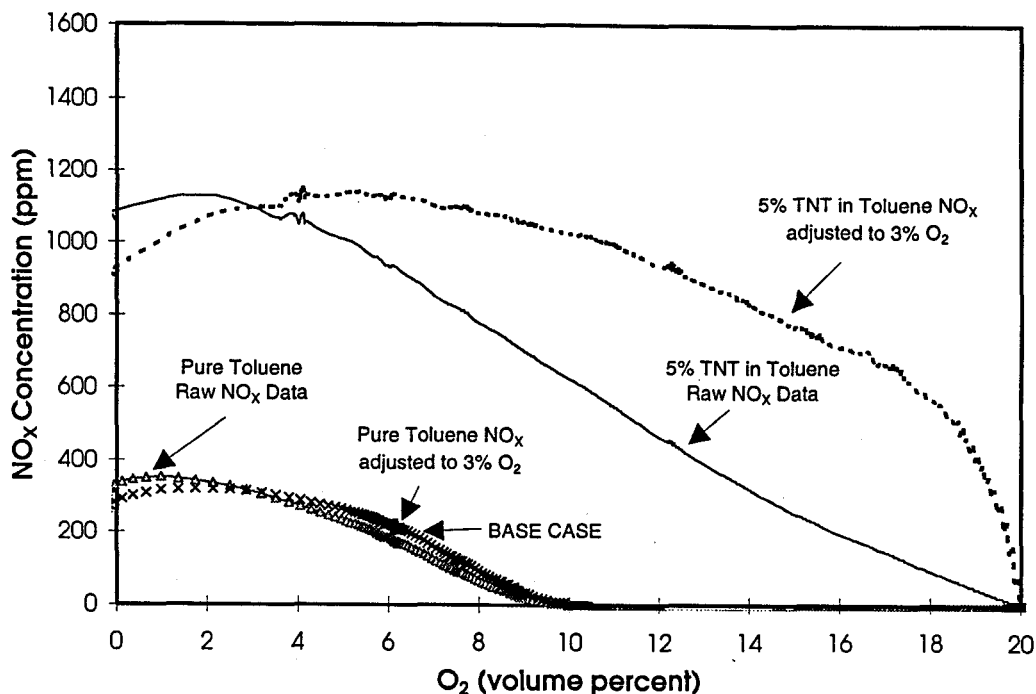


Figure 6. Measurements of  $\text{NO}_x$  concentrations of pure toluene and 5% (by weight) TNT in toluene, with a residence time of 3.8 seconds and wall temperatures held at  $900^\circ\text{C}$ .

To fully understand the  $\text{NO}_x$  generation from EMDF containing nitrate groups, it would be helpful to be able to determine the yield of each of the source mechanisms for  $\text{NO}_x$  formation (i.e. thermal, prompt, and fuel-bound nitrogen). The similarities in the molecular structure of TNT and toluene allow us to make the simplification that the addition of TNT to toluene adds fuel- $\text{NO}_x$  formation from the TNT, while the prompt and thermal  $\text{NO}_x$  concentrations remain equal to the prompt and fuel  $\text{NO}_x$  formed from toluene alone. This is equivalent to the approximation that the fuel-nitrogen mechanism does not interact with the prompt and thermal  $\text{NO}_x$  mechanisms. Ignoring interactions will somewhat overpredict  $\text{NO}_x$  concentrations, as  $\text{NO}_x$  formation is strongly influenced by  $\text{NO}_x$  concentrations due to reactions such as  $\text{NO} + \text{NO} \Rightarrow \text{N}_2 + \text{O}_2$ , but this approach will give an idea of the order of magnitude of the fuel  $\text{NO}_x$  produced from TNT.

Figure 7 recasts the data of Figure 6 to show the  $\text{NO}_x$  formation due to the fuel-bound nitrogen for the TNT EMDF. The toluene and 5% TNT in toluene  $\text{NO}_x$  data corrected to 3% oxygen are shown. The shaded area on the graph, equal to the nitrogen oxide concentrations produced during pure toluene combustion, roughly represents the

NO<sub>x</sub> produced by thermal and prompt mechanisms during the combustion of 5% TNT in toluene. The remaining area under the 5% TNT in toluene curve, after subtracting the shaded area, represents the NO<sub>x</sub> formed from fuel-bound nitrogen. Comparing this with the dotted line at the top of the graph, which is the calculated NO<sub>x</sub> concentration if all of the nitrogen in the TNT were converted completely to nitrogen oxides, it is apparent that through the entire range of oxygen concentrations (0-18%), at least 50% of the fuel nitrogen is converted directly to NO<sub>x</sub>. Similar arguments hold for the double-base propellant shown in Fig. 5. In Fig. 7, the peak in the fuel-nitrogen contribution at approximately 10% O<sub>2</sub> is explained by the fact that at lower oxygen concentrations there is more competition for O<sub>2</sub>, favoring the reduction of some of the nitrogen oxides to N<sub>2</sub>O or N<sub>2</sub>. The fall-off of fuel NO<sub>x</sub> concentrations at oxygen concentrations higher than 10% is due to decreasing flame temperature with increasing O<sub>2</sub> concentration, as well as the possibility that at more dilute fuel concentrations less complete combustion is taking place, and another breakdown pathway in addition to C-N homolysis is becoming important.

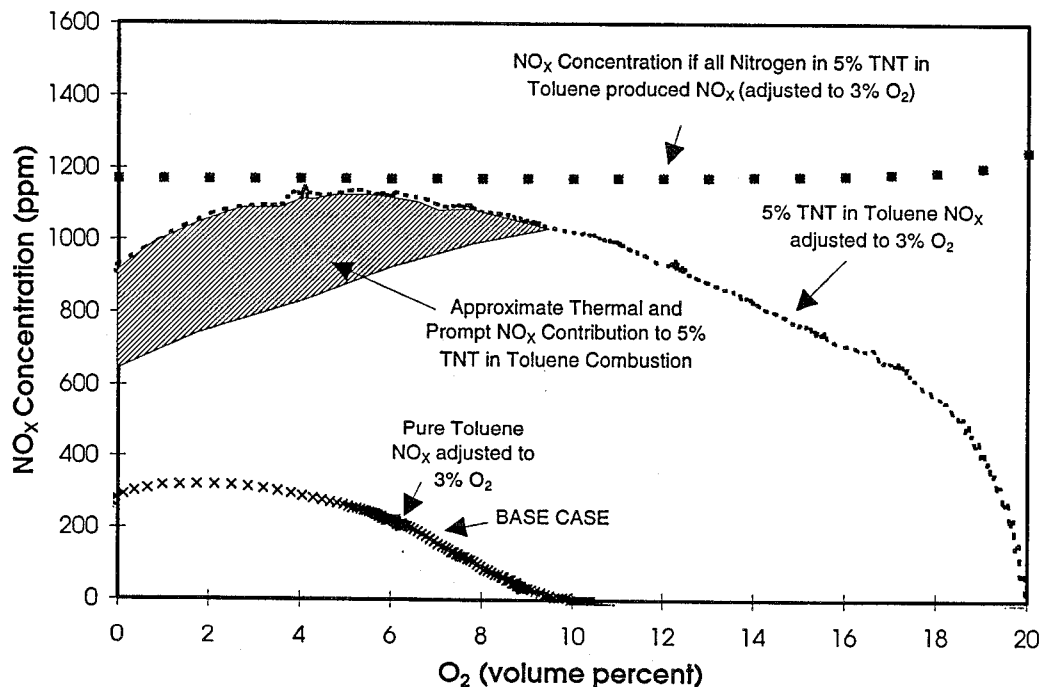


Figure 7. NO<sub>x</sub> concentrations from combustion of pure toluene and 5% TNT in toluene, adjusted to 3% oxygen, showing the contribution of thermal and prompt NO<sub>x</sub>, as well as the total potential contribution of fuel nitrogen from the TNT.

Direct formation of nitrogen oxides from fuel-bound nitrates contrasts with  $\text{NO}_x$  formation from most nitrogen-containing fuels. Specifically,  $\text{NO}_x$  formation from most fuels proceeds through a reaction pathway involving HCN and  $\text{NH}_x$  as intermediates, with overall conversion favoring molecular nitrogen. Both the TNT data and the double-base propellant data indicate fuel nitrogen conversion efficiencies that are high compared to traditional fuels. The interpretation of these data is that  $\text{NO}_x$  is formed directly during thermal decomposition of these fuels, without proceeding through HCN or other intermediates, as illustrated in Fig. 2. This aspect of the combustion behavior of EMDFs sets them apart from essentially all other nitrogen-containing solid fuels. These results are consistent with thermal decomposition data on RDX and HMX, two other EM with bound nitrate groups (Behrens Jr. 1990; Behrens Jr. and Bulusu 1991; Behrens Jr. and Bulusu 1992; Behrens Jr. and Bulusu 1992). A portion of the resulting  $\text{NO}_x$  likely further reacts to form  $\text{N}_2$ , consistent with established  $\text{NO}_x$  kinetics.

Figure 8 shows  $\text{NO}_x$  data from the combustion of an emulsion of 5% (by weight) nitroguanidine in fuel oil #2, compared with  $\text{NO}_x$  data from firing the fuel oil alone. When fired alone, the fuel oil was fired using the positive displacement feeder. Nitroguanidine, the structure of which is shown in Figure 1, has only a single  $\text{NO}_2$  group, two NH groups, and an  $\text{NH}_2$  group, and is thus very different from the previous two fuels. Combustion of both the double-base propellant (Fig. 5) and the 5% TNT fuel (Fig. 6) shows that the nitrate groups are readily converted to  $\text{NO}_x$ . However, the direct nitrate conversion to  $\text{NO}_x$  is somewhat less efficient in the case of nitroguanidine; if only the  $\text{NO}_2$  on the nitroguanidine molecule were converted to NO, the resulting concentration would be 713 ppm when nitroguanidine is fired at 2% excess  $\text{O}_2$ . If all of the fuel nitrogen were converted into  $\text{NO}_x$ , the resulting concentration would be 2,850 ppm in the product gases, which is far above both the equilibrium and the measured value. In this case, the peak measured value of  $\text{NO}_x$  concentration is roughly 380 ppm, which is roughly half of the nitrate-bound nitrogen, or 13% of the total fixed nitrogen. These lower levels of conversion of nitrogen to  $\text{NO}_x$  suggest that more traditional nitrogen chemistry routes are dominant for nitroguanidine, consistent with the smaller fraction of fuel-bound nitrogen present as  $\text{NO}_2$  in this material.

Figure 9 illustrates  $\text{NO}_x$  data for polybutadiene rocket binder material mixed with coal at a 65:35 mass ratio. The rocket binder material has no  $\text{NO}_2$  groups; the small amount of fuel nitrogen present in the fuel is in the form of ammonium perchlorate residual. The intent is to remove all of the  $\text{NH}_4\text{ClO}_4$  during the pretreatment, but inevitably a small

amount remains in the treated fuel. Once blended with coal, total fuel nitrogen originates approximately 50% from the coal and 50% from the binder. In its raw form, the binder material is a porous, adherent, rubber material that is difficult to handle. It cannot be maintained at reasonably small particle sizes without coating it with a powder or similar material to prevent reagglomeration. Per mass of fuel, observed  $\text{NO}_x$  concentrations from the binder material are much lower than those for double-base material (Fig. 5) and the TNT (Fig. 6), consistent with the lower nitrogen content of the fuel (0.04 mass percent) and the mode of occurrence of nitrogen. Further, in the next section we will suggest that the  $\text{NO}_x$  formation route for this material is substantially different than that for the earlier EMDF containing nitrate groups.

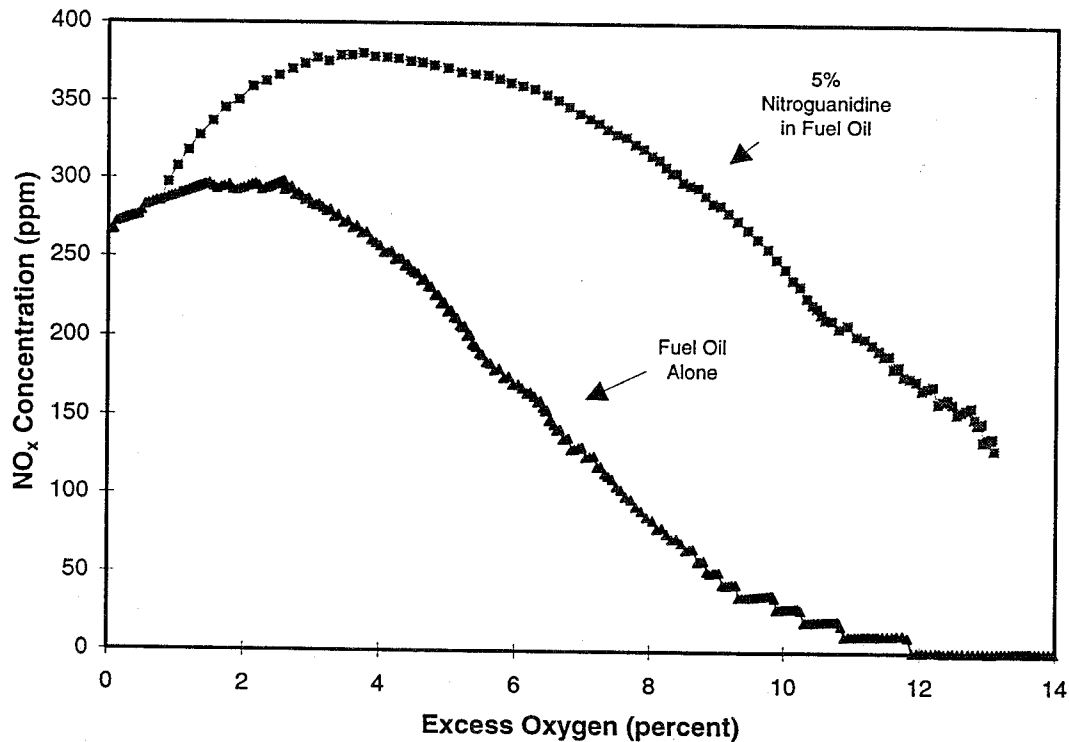


Figure 8. Measurements of  $\text{NO}_x$  concentrations of 5% (by weight) nitroguanidine in fuel oil #2, with a combustor residence time of 3.8 seconds and wall temperatures held at 900 °C.

## Influence of Aluminum on Combustion Process

The polybutadiene material is impregnated with flakes of aluminum to increase the specific impulse of the propellant. Experiments in both the MFC and the CCL indicate that aluminum particle temperatures are extremely high during rocket binder combustion.

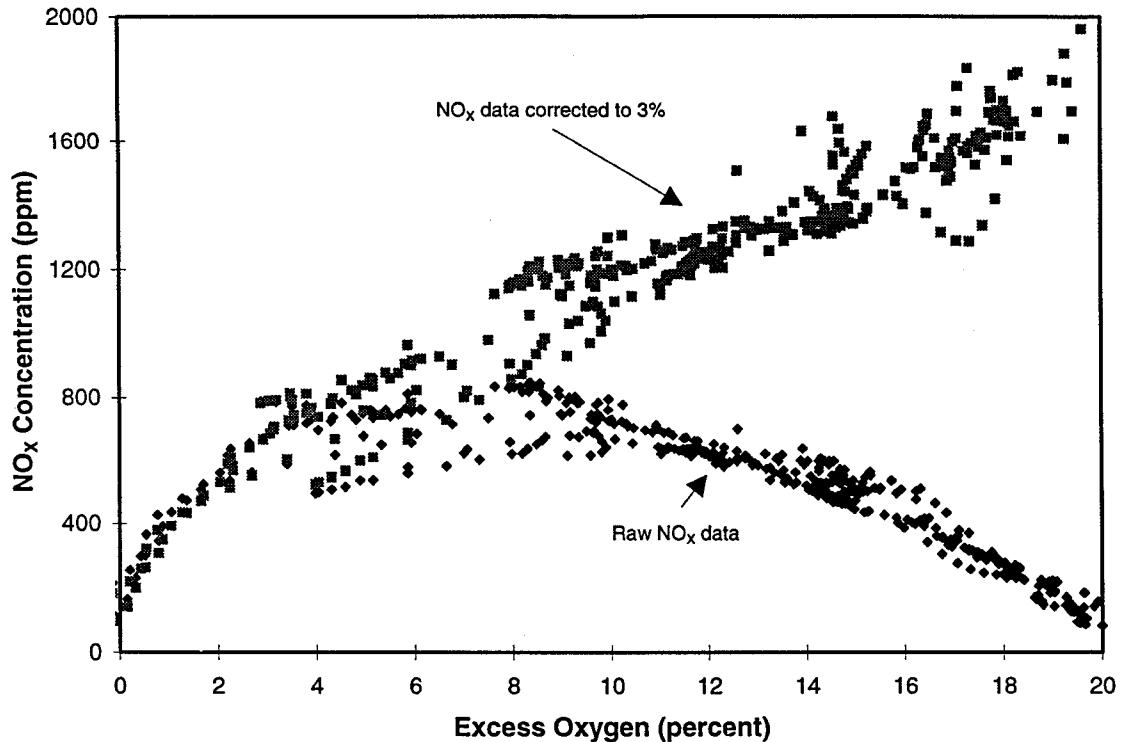


Figure 9. NO<sub>x</sub> emissions from the polybutadiene rocket propellant binder material mixed in a 65:35 mass ratio with coal, as a function of exit O<sub>2</sub> concentration and atomizing air to combustion air flow rates.

In the CPI we have an optical temperature measurement system that is calibrated up to 1700 °C. Single particle combustion experiments were conducted in environments with oxygen concentrations ranging from 1% O<sub>2</sub> to 20% O<sub>2</sub>. Under all conditions, the particle temperature exceeded the upper limit of our diagnostic. During 12% O<sub>2</sub> experiments in the CPI, the particles melted through the alumina mat used to hold them. The Al<sub>2</sub>O<sub>3</sub> melting point is approximately 2000 °C, depending on crystalline structure. At 6% O<sub>2</sub>, the temperature was again higher than 1700 °C, but the particles did not melt

through the mat. Coating of particles with coal seemed to reduce their temperatures, but never below 1700 °C. Observations at the remaining oxygen concentrations were made in the MFC and particle temperatures were very high judging from particle emission, but particles were not stationary during individual shutter cycles so no reliable temperature measure could be made.

These high temperatures are believed to induce significant  $\text{NO}_x$  formation through the thermal formation mechanism. Experimental evidence of this is found by blending varying ratios of coal and EMDF and analyzing the trend in the  $\text{NO}_x$  data, shown in Figure 10.

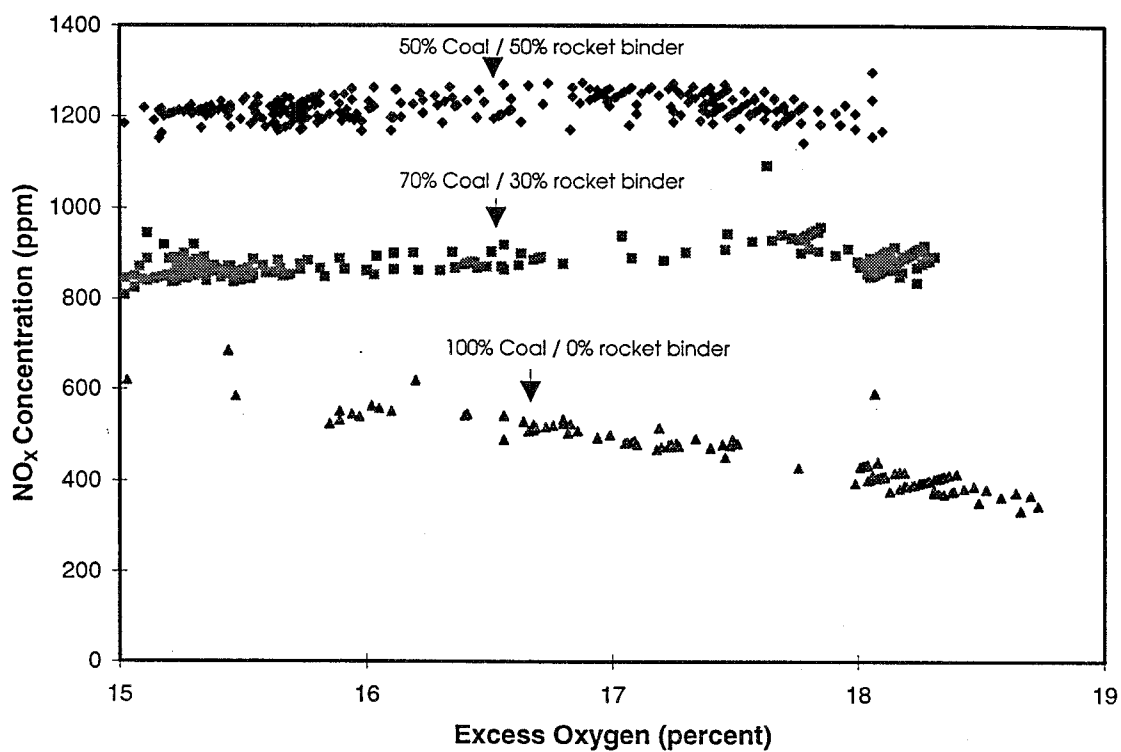


Figure 10. Measured  $\text{NO}_x$  concentrations with changes in coal content for a blend of polybutadiene rocket binder-derived EMDF and coal.

Coal, which in this case contains about 0.75% fuel nitrogen, is the dominant fuel nitrogen-containing portion of the blend. The only fuel nitrogen in the EMDF is in trace amounts associated with residual ammonium perchlorate. If fuel nitrogen is the primary source of  $\text{NO}_x$ , increases in coal content should increase  $\text{NO}_x$ . The observed trend is the opposite (Fig. 8), supporting the supposition that the dominant formation mechanism for  $\text{NO}_x$

during combustion of rocket motor binder is thermal. These data were obtained at high oxygen concentrations (low particle loadings) to minimize complications of changing flame structure with changes in blend ratio. At these high oxygen concentrations, there is no well-defined flame front or fireball, and hence combustion occurs mainly around individual particles.  $\text{NO}_x$  is believed to form primarily due to the high temperatures surrounding the aluminum-containing particles.

Our results also indicated that molten aluminum particles exist in flows well after 1.5 s of residence time. This sustained presence of molten material presents some deposition threat to a boiler system. In addition, the large amount of inorganic material in the fuel (the binder is 60% aluminum by weight) could overwhelm particulate cleanup systems if a high percentage of this EMDF were fired in a boiler. Model predictions of metal-containing energetic material cofiring conclude that the behavior of ash is the limiting factor in the amount of energetic material that can be blended with coal for the particular system considered (Li, Sheldon et al. 1995). The potential for particle deposition and damage to grates or other equipment from aluminum are concerns in the reapplication of energetic materials as fuels, but this issue can be managed by blending the aluminum-containing EMDF with other fuels and by judiciously choosing the boiler design and operating conditions with which to treat the material. Careful management of the fuel on a grate or in a kiln or combustion in suspension, as in an entrained-flow system, should prevent damage to systems at commercial scale.

### **$\text{NO}_x$ Control Strategies**

Due to the high levels of  $\text{NO}_x$  generated by EMDF combustion, it is crucial to demonstrate that commonly used  $\text{NO}_x$  control measures such as staged combustion, reburning, selective non-catalytic reduction (SNCR) and selective catalytic reduction (SCR) will be able to adequately reduce the  $\text{NO}_x$  concentrations. This requires that the nitrogen from the fuel be converted to the gas-phase relatively early in the combustion process, as each of these methods rely on controlling the gas-phase chemistry to reduce the  $\text{NO}_x$  formation (as in the case of staged combustion), to convert  $\text{NO}_x$  already formed to  $\text{N}_2$  (as in SNCR and SCR), or both (as in reburning). We have chosen to demonstrate  $\text{NO}_x$  control using staged combustion, the simplest method of the four. Staged combustion works by burning the fuel in two distinct stages. The first stage is burned fuel-rich; the lack of excess oxygen in this stage promotes the fuel-bound nitrogen to form  $\text{N}_2$  instead of  $\text{NO}$ , but also leaves a significant portion of the carbon not fully reacted (i.e. as  $\text{CO}$  instead of  $\text{CO}_2$ , for example). At the beginning of the second stage, excess air is

injected, and the second stage burns fuel-lean. This completes the conversion of carbon to  $\text{CO}_2$  while keeping the temperatures low, thus not promoting thermal  $\text{NO}_x$  formation. A question at the outset of this investigation was whether or not the first stage would be effective in converting the fuel-bound nitrogen to  $\text{N}_2$ , when the nitrogen was present in the form of nitrates.

To look at the effect of chemistry on  $\text{NO}_x$  concentrations, a series of axial  $\text{NO}_x$  measurements from firing toluene and 5% TNT in toluene were taken. As expected for both fuel mixtures, nitrogen oxide concentrations peak in the high-temperature flame region and then decrease toward their equilibrium value in the cooled gases downstream. For all of the TNT runs the  $\text{NO}_x$  concentrations near the flame exceed the range of the meter (1500 ppm). Figure 11 illustrates axial  $\text{NO}_x$  concentration data from toluene combustion, which are qualitatively similar to the TNT/toluene  $\text{NO}_x$  data, at various excess oxygen concentrations.

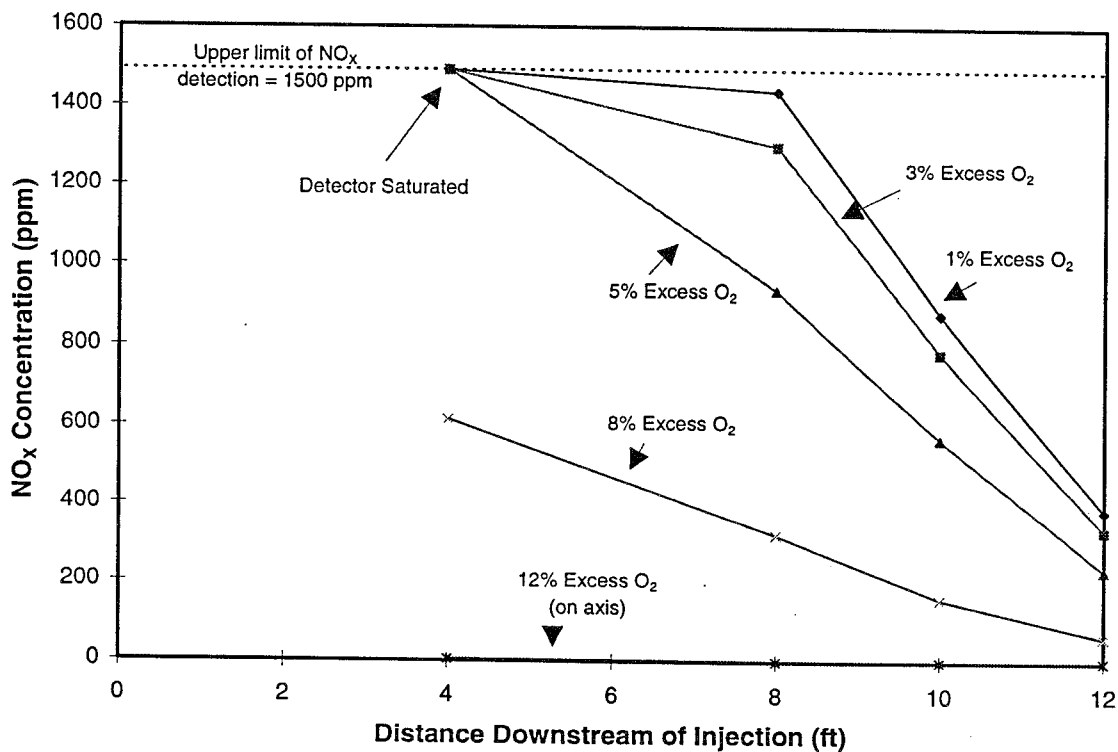


Figure 11. Axial  $\text{NO}_x$  concentration data from toluene combustion at various excess oxygen concentrations, normalized to 3% excess oxygen.

We do not expect significant radial gradients in the NO<sub>x</sub> concentration, despite the fact that the Reynolds number is fairly low (1500), as the fuel spray is sufficiently dispersed. The data for 1% and 3% excess oxygen fall almost exactly on top of each other, while the data for 12% excess oxygen shows nearly zero measured NO<sub>x</sub> along the entire length of the combustor. Under all conditions the nitrogen oxide concentrations decrease monotonically following the high concentrations in the flame as the gases approach the wall temperature (900 °C). At higher excess oxygen concentrations less NO<sub>x</sub> is formed in the toluene flame, primarily due to lower flame temperatures. However, at the higher excess oxygen concentrations the NO<sub>x</sub> removal rate also decreases, as the excess oxygen lowers the rate of removal reactions such as  $\text{NO} + \text{NO} \Rightarrow \text{N}_2 + \text{O}_2$  by Le Chatelier's principle. These measurements show the effect of equivalence ratio on both the NO<sub>x</sub> production and the rate of NO<sub>x</sub> removal, both of which are important for understanding the staged burning technique. The fact that virtually no NO<sub>x</sub> is formed at the 12% excess O<sub>2</sub> condition shown in Figure 11 shows that the lower temperatures associated with lean combustion prevent the formation of thermal NO<sub>x</sub>.

Table 2. NO<sub>x</sub> concentration data from combustion tests of staged and unstaged toluene and 5% TNT in toluene.

Excess Oxygen (percent)	Unstaged 5% TNT NO <sub>x</sub> (ppm)	Staged 5% TNT NO <sub>x</sub> (ppm)	Percent Reduction for TNT / Toluene	Excess Oxygen (percent)	Unstaged Toluene NO <sub>x</sub> (ppm)	Staged Toluene NO <sub>x</sub> (ppm)	Percent Reduction for Toluene
3	1080	420	61%	1	310	180	42%
5	1110	415	63%	2.2	320	260	19%
7	1090	400	63%	4	280	240	14%
9	1060	380	64%	6	215	170	21%
				8	100	50	50%

Table 2 shows results from staged-burning experiments with the 5% TNT in toluene mixture as well as with pure toluene. In these experiments, the fuel was injected

at the top of the combustor, air was injected 1.8 meters downstream of the fuel injection (1.4 seconds residence time), and gas measurements were taken 3.66 meters downstream of the fuel injection. In all cases, the first stage was run at a constant (fuel-rich) equivalence ratio of 1.3 and the amount of air injected into the second stage was varied. The variation of air flowrate to the second stage means that the residence time in the second stage changes somewhat, but visual observations would suggest that much of the important chemistry takes place at the beginning of the second stage, in the first 0.5 meter after secondary air injection, where the fuel burns out. Data corrected to 3% oxygen are shown for a given excess oxygen concentration at the bottom of the combustor, either with or without air staging. For both fuels there is a marked decrease in the  $\text{NO}_x$  levels associated with staged combustion. For the pure toluene mixture the fractional decrease in  $\text{NO}_x$  concentration is greatest at the highest and lowest excess oxygen concentrations, in keeping with the fact that most of the  $\text{NO}_x$  is thermally generated; at 8% excess oxygen concentration the staging reduces the  $\text{NO}_x$  by a factor of 2, to a value of 50 ppm. For the 5% TNT in toluene mixture the effect of staged combustion remained relatively constant across a range of excess air values, showing in all cases nearly a threefold reduction in  $\text{NO}_x$  over the unstaged values. This indication of significant  $\text{NO}_x$  reduction via staging demonstrates that this and related combustion process techniques will be able to successfully mitigate the  $\text{NO}_x$  emissions for EMDF, as they do for traditional fuels.

### **Other Issues**

In addition to  $\text{NO}_x$  issues and the behavior of aluminum, the possible formation of air toxics is an issue for the combustion of energetic material-derived fuels. Air toxics are conveniently discussed in the categories of inorganic and organic toxics and are delineated in the 1990 amendment to the Clean Air Act (1989). Inorganic toxics of relevance to combustion of energetic material derived fuels include beryllium, lead, and trace or impurity amounts of other toxic inorganics. We have analyzed representative samples of energetic materials for their total inorganic concentrations using neutron activation analysis (NAA). The concentrations are near or below detection limits for all of the compounds and samples analyzed thus far, none of which include either lead or beryllium as intentionally added materials. EMDFs containing either lead or beryllium in more than impurity concentrations (ppm or less) are poor candidates for use as fuels.

Organic air toxics of principal concern include chlorinated aromatic hydrocarbons in the forms of dioxins, furans, polychlorinated biphenyls (PCBs), or their precursors. There is a possibility of the formation of these compounds when fuels including residual

chlorine are used, such as binders from ammonium perchlorate-based rocket motors. Because chlorinated aromatic compounds are rare in the fuel, the formation of the compounds, if any, would occur as combustion gases cool in the post-flame environment. This issue has been addressed for incineration of these materials (Biagioni Jr. 1994), but has not been addressed in combustion or power generation systems. In Biagioni's work, the total production of furans and dioxins was below regulatory limits. We anticipate similar results for power generating combustion systems and are continuing work in this area to validate our conjecture.

## CONCLUSIONS

The potential for reapplication of excess energetic materials as boiler fuels has been economically and experimentally explored. The economics suggest that the cost of such disposal techniques could be approximately equivalent to the cost of constructing and operating the facility that removes the material and desensitizes it. Revenues gained from power generation and chemical recovery are approximately equal to expenses of boiler modifications and operation and maintenance of new feedlines.

One of the primary combustion issues surrounding EMDF is the formation of pollutants, especially  $\text{NO}_x$ . In the near-term, the success of EMDF as supplemental boiler fuels depends in large part on the degree to which proven  $\text{NO}_x$ -control combustion technologies can be applied to reduce emissions.  $\text{NO}_x$  emissions from combustion of EMDF containing bound nitrate groups are notably higher than from combustion of traditional fuels with similar nitrogen contents. The data suggest that thermal decomposition of the EMDF leads to direct, quantitative formation of  $\text{NO}_x$  from the fuel nitrogen bound in nitrate groups. We have shown that staged burning effectively reduced the  $\text{NO}_x$  levels in our pilot-scale system, demonstrating that the  $\text{NO}_x$  formed from EMDF should be treatable by the same down-stream treatment techniques as are effective with other fuels. Thus, we expect that were EMDF blended with traditional fuels in a 10% blend, for example,  $\text{NO}_x$  emissions from EMDF would not be prohibitive if staged combustion or a similar technique such as reburning, SCR, or SCNR were applied.

A second important combustion-related issue for EMDF containing energetic metals such as aluminum is the extremely high temperatures we found the aluminum-containing particles to reach in our experiments. Aluminum particles attain temperatures in excess of 2000 °C, well above the melting point of aluminum, and remain at high

temperatures for 1.5 s or more, which is long compared to residence times available in the furnace sections of most commercial boilers. We found that on a per-mass-of-fuel basis, NO<sub>x</sub> emissions from rocket propellant binders containing aluminum are much lower than for EMDF containing nitrate groups, but still are appreciable. The data suggest much greater contributions from thermal mechanisms, likely due to these high particle temperatures. The potential for particle deposition and damage to grates or other equipment from aluminum is a concern in the reapplication of energetic materials as fuels, but we believe that this issue can be managed by blending the EMDF with other fuels and by judiciously choosing the boiler design and operating conditions with which to treat the material. Careful management of the fuel on a grate or in a kiln or combustion in suspension may prevent damage to commercial-scale systems. The ash formed after complete combustion is benign and should not pose a problem for any combustor except in quantity.

## ACKNOWLEDGMENTS

Funding for this work was provided by Sandia National Laboratories' Laboratory-directed Research and the US Government's Strategic Environmental Research and Development Program (SERDP). Contributions in the form of energetic materials for testing, desensitization of such materials, and laboratory characterization and transportation certification were made by Indian Head Naval Surface Warfare Center (Indian Head), Thiokol Corp., Alliant TechSystems, and Global Environmental Solutions. The authors gratefully acknowledge Tim Dunn (Indian Head), Louis Kanaras (SERDP and US Army Environmental Center, Aberdeen Proving Ground), Jim Persoon (Alliant TechSystems), Kevin Farnsworth (Global Environmental Solutions), and John Slaughter and Bill Munson (Thiokol Corp.) for their financial support, technical comments, and cooperation in obtaining energetic materials.

The authors also acknowledge the contributions of many colleagues at Sandia, most notably Allen Robinson, Joel Lipkin, Jack Swearingen, Donald Hardesty, and Howard Hirano, in managing this project and critiquing our results.

## REFERENCES

- (1989). Federal Register: Part III; Air Contaminants.
- Arbuckle, J. (1996). Conventional Ammunition Demilitarization Program. 4th Global Demil Symposium, Sparks, NV.

Behrens Jr., R. (1990). "Thermal Decomposition of Energetic Materials: Temporal Behaviors of the Rates of Formation of the Gaseous Pyrolysis Products from Condensed-Phase Decomposition of Octahydro-1,3,5,7-tetranitro-1,3,5,7-tetrazocine." Journal of Physical Chemistry **94**(17): 6706-6718.

Behrens Jr., R. and S. Bulusu (1991). "Thermal Decomposition of Energetic Materials: 2. Deuterium Isotope Effects and Isotopic Scrambling in Condensed-Phase Decomposition of Octahydro-1,3,5,7-tetranitro-1,3,5,7-tetrazocine." Journal of Physical Chemistry **95**(15): 5838-5845.

Behrens Jr., R. and S. Bulusu (1992). "Thermal Decomposition of Energetic Materials. 3. Temporal Behaviors of the Rates of Formation of the Gaseous Pyrolysis Products from Condensed-Phase Decomposition of 1,3,5-Trinitrohexahydro-s-triazine." Journal of Physical Chemistry **96**(22): 8877-8891.

Behrens Jr., R. and S. Bulusu (1992). "Thermal Decomposition of Energetic Materials. 4. Deuterium Isotope Effects and Isotopic Scrambling (H/D,  $^{13}\text{C}/^{18}\text{O}$ ,  $^{14}\text{N}/^{15}\text{N}$ ) in Condensed-Phase Decomposition of 1,3,5-Trinitrohexahydro-s-triazine." Journal of Physical Chemistry **96**(22): 8891-8897.

Biagioni Jr., J. R. (1994). "Development of an Environmentally Acceptable Thermal Treatment Alternative for Energetic Material." Hazardous Waste and Hazardous Materials **11**(1): 217-226.

Blixrud, C. M. (1996). Demilitarization in the Former Soviet Union. 4th Global Demil Symposium, Sparks, NV.

Cor, J. J. and M. C. Branch (1995). "Structure and Chemical Kinetics of Flames Supported by Solid Propellant Combustion." Journal of Propulsion and Power **11**(4): 704-716.

Huizinga, M. (1996). Industry/Government Panel on Conventional Ammunition Demilitarization. 4th Global Demil Symposium, Sparks, NV.

Li, B. W., M. S. Sheldon, et al. (1995). Feasibility of Cofiring Waste Solid Rocket Propellants with Coal. Joint Meeting of the American Flame Research Foundation and the Western States, Central States, and Mexican Sections of the Combustion Institute, San Antonio, TX.

Melius, C. F. (1988). The Gas-Phase Chemistry of Nitramine Combustion. 25th JANNAF Combustion Meeting.

Melius, C. F. (1990). Thermochemical Modeling: II Application to Ignition and Combustion of Energetic Materials. Chemistry and Physics of Energetic Materials. S. N. Bulusu. Norwell, MA, Kuwer Academic: 51-78.

Miller, J. A. and C. T. Bowman (1989). "Mechanism and Modeling of Nitrogen Chemistry in Combustion." Progress in Energy and Combustion Science **15**: 287-338.

Myler, C. A., W. M. Bradshaw, et al. (1991). "Use of Waste Energetic Materials as a Fuel Supplement in Utility Boilers." Journal of Hazardous Materials **26**: 333-342.

Shah, D. S. (1994). Analysis of Propellants, Explosives, and Pyrotechnics Co-Combustion in Fossil Fuel and Biomass Boilers as Means of Resource Recovery and Recycle, White Paper, Sandia National Laboratories.

Sierra (1996). Personal Communications with Sierra Army Depot Staff.

Steele (1996). Solid Rocket Motor Contained Burn Process. 4th Global Demil Symposium, Sparks, NV.

Wheeler, J. (1996). Opening Remarks. 4th Global Demil Symposium, Sparks, NV.

Wilcox, J. L. (1996). OB/OD Emissions Characterization. 4th Global Demil Symposium, Sparks, NV.

UNLIMITED RELEASE  
INITIAL DISTRIBUTION

Ms. Alice Atwood  
Physical Scientist  
Engineering Sciences Division  
Research Department  
China Lake, CA 93555-6001

Dr. Michael Berman  
AFOSR  
AFOSR/NC  
Bolling AFB, DC 20332

Dr. Thomas Boggs  
Naval Weapons Center  
Code 389  
China Lake, CA 93555

Dr. Surya N. Bulusu  
ARDEC  
SMCAR-AEE-WW  
Dover, NJ 07801-5001

Dr. Robert D. Chapman  
Naval Air Warfare Center  
Code 464220D  
China Lake, CA 93555

Dr. Ronald L. Derr  
Naval Weapons Center  
Code 389  
China Lake, CA 93555

John Dow  
Naval Surface Warfare Center  
Indian Head Division  
Energetic Mat. Res. & Tech. Dpt.  
Indian Head Division, NSWC  
Indian Head, MD 20640-5035

Dr. David S. Downs  
ARDEC  
SMCAR-AEE-B  
Dover, NJ 07801-5001

Timothy J. Dunn  
Naval Surface Warfare Center  
Indian Head Division  
Energetic Mat. Res. & Tech. Dpt.  
Indian Head Division, NSWC  
Indian Head, MD 20640-5035

Doug Elstrodt  
Naval Surface Warfare Center  
Code 9130  
Energetic Materials Chemistry Division  
Indian Head, MD 20640-5035

Dr. Robert A. Fifer  
Ballistic Research Laboratory  
SLCBR-IB-I  
Aberdeen Proving Ground, MD 21005-5066

Brad Forch  
Ballistic Research Laboratory  
SLCBR-IB-I  
Aberdeen Proving Ground, MD 21005-5066

Dr. Arpad A. Juhsz  
Ballistic Research Laboratory  
SLCBR-IB-B  
Aberdeen Proving Ground, MD 21005-5066

Louis Kanaras  
US Army Env. Center  
Env. Technology Division  
Tech. Demon. & Transfer Branch  
Aberdeen Proving Ground, MD 21010-5401

Dr. Solim S. Kwak  
Demil Technology Office  
Defense Ammunition Center & School  
SIOAC-TD  
Savanna, IL 61074-6939

Dr. J.A. Lannon  
U.S. ARDEC  
Dover, NJ 07801-5001

Dr. Donald Liebenberg  
U.S. Office of Naval Research  
800 N. Quincy St.  
Arlington, VA 22217

Dr. David M. Mann  
U.S. Army Research Office  
PO Box 12211  
Research Triangle Park, NC 27709-2211

Walter Marx  
Naval Surface Warfare Center  
Indian Head Division  
Energetic Mat. Res. & Tech. Dpt.  
Indian Head Division, NSWC  
Indian Head, MD 20640-5035

Dr. Ingo W. May  
Ballistic Research Laboratory  
SLCBR-IB-B  
Aberdeen Proving Ground, MD 21005-5066

Dr. Robert L. McKenney, Jr.  
Energetic Materials Branch  
WL/MNME  
Englin Air Force Base, FL 32542-5434

Dr. Richard S. Miller  
Office of Naval Research  
800 North Quincy St.  
Arlington, VA 22217

Dr. Tim Parr  
Naval Air Warfare Center  
Code CO2392  
China Lake, CA 93555-6001

Betsy Rice  
Ballistic Research Laboratory  
SLCBR-IB-I  
Aberdeen Proving Ground, MD 21005-5066

Dr. Robert W. Shaw  
U.S. Army Research Office  
PO Box 12211  
Research Triangle Park, NC 27709

Mr. Benjamin Stokes  
Technical Officer-Propulsion Effects  
USNATO/IS  
PSC 81 Box 16  
APO, AE 09724

Rose Tesce-Rodriguez  
Ballistic Research Laboratory  
SLCBR-IB-I  
Aberdeen Proving Ground, MD 21005-5066

James Q. Wheeler  
Demil Technology Office  
Defense Ammunition Center & School  
SIOAC-TD  
Savanna, IL 61074-6939

Merrill Beckstead, Professor  
Brigham Young University  
Chemical Engineering Dpt.  
350 Clyde Building  
Provo, UT 84602

Professor Melvyn C. Branch  
University of Colorado  
Department of Mechanical Eng.  
Boulder, CO 80309-0427

Professor M. Quinn Brewster  
University of Illinois  
Dept. of Mech. and Indus. Eng.  
Urbana, IL 60801

Professor Thomas B. Brill  
University of Delaware  
Department of Chemistry  
Newark, DE 19711

Professor Thomas Litzinger  
The Pennsylvania State University  
Department of Mechanical Eng.  
University Park, PA 16802

Candace Morey  
Cornell University  
125 N. Quarry St. Apt #3  
Ithaca, NY 14850

Professor Jimmie C. Oxley  
Department of Chemistry  
New Mexico Institute of Mining and  
Technology  
Socorro, NM 87801

Jerry Cole  
Energy & Environmental Research  
18 Mason  
Irvine, CA 92718

Dr. Marc DeFourneaux  
Project Manager  
NIMIC  
International Staff  
NATO-1110  
Brussels, Belgium

Kevin Farnsworth  
Global Environmental Solutions, Inc.  
4100 South 8400 West  
Annex 16  
Magna, UT 84044-0098

Stan Harding  
Reaction Engineering International  
77 West 200 South  
Suite 210  
Salt Lake City, UT 84101

Leon Hyde  
Thiokol  
PO Box 689  
MS 130  
Brigham City, UT 84302-0689

Kathy Miks  
Thiokol Corporation  
MS 243  
Brigham City, UT 84302

Bill Munson  
Thiokol Corporation  
MS 300  
Brigham City, UT 84302

John Slaughter  
Thiokol Corporation  
MS 300  
Brigham City, UT 84302

Hap Stoller  
TPL, Inc.  
3768 Hawkins St. NE  
Albuquerque, NM 87109

Dr. Larry Waterland  
Acurex Corp.  
Environmental Systems Division  
485 Clyde Ave  
PO Box 1044  
Mountain View, CA 94039

Cesar Preneda  
University of California  
Lawrence Livermore National Laboratories  
7011 East Ave.  
Livermore, CA 94550

L-282 R. Atkins

L-282 J. Maienschein

L-282 C.O. Pruneda

MS0828 R.D. Skocypec, 1102

MS1454 A.M. Renlund, 1514

MS1452 J. G. Harlan, 1552

MS1454 L.L. Bonzon, 1554

MS0188 C. Meyers, 4523

MS9001 T.O. Hunter, 8000  
Attn: 8100 M.E. John  
8200 L.A. West  
8400 R.C. Wayne  
8800 P.E. Brewer

MS9056 L. Thorne, 8120

MS9163 W. Bauer, 8302

MS9052 S.W. Allendorf, 8361

MS9052 R. Behrens, 8361

MS9052 L.L. Baxter, 8361

MS9052 S.G. Buckley, 8361 (5)

MS9052 D.R. Hardesty, 8361 (10)

MS9052 M.M. Lunden, 8361

MS9052 S.F. Rice, 8361

MS9052 J.R. Ross, 8361

MS9052 G.C. Sclippa, 8361

MS9052 C. Shaddix, 8361

MS9105 H. Hirano, 8419

MS0834 K.L. Erickson, 9112

MS0834 M.L. Hobbs, 9112

MS9021 Technical Communications  
Department, 8535, for OSTI

MS9021 Technical Communications  
Department, 8535/Technical  
Library, MS0899, 13414

MS0899 Technical Library, 13414 (4)

MS9018 Central Technical Files, 8523-2